

Integrating Adam Optimizer to Enhance Efficiency of Transfer Learning Model for Diagnosing Cancers

Sushree Gayatri Priyadarsini Prusty¹, Narayan Patra², Sashikanta Prusty^{1*}, Jyotirmayee Rautaray³, Ghanashyam Sahoo⁴

¹Department of Computer Science & Engineering,
Siksha 'O' Anusandhan University,
Bhubaneswar-751030, India
liza.sushree19@gmail.com

²Department of Computer Science & Information Technology,
Siksha 'O' Anusandhan University,
narayanpatra@soa.ac.in

³Department of Computer Science & Engineering,
Siksha 'O' Anusandhan University,
Bhubaneswar-751030, India

Correspondence: sashi.prusty79@gmail.com

⁴Department of Computer Science & Engineering,
Odisha University of Technology and Research,
Bhubaneswar, India
jyotirmayee.1990@gmail.com

⁵Department of Computer Science & Engineering,
GITA Autonomous College,
Bhubaneswar, India
ghanarvind@gmail.com

Abstract— Introduction: Despite huge advancements in medical fields, diseases like cancer continue to plague people since we are still prone to them. The main purpose is to design a critical analysis of cancers, including breast, pancreatic, colon, skin, lung, and other cancers from the year 1990 to 2019, to identify some of the rising factors of both lung and colon cancers that cause unnecessary deaths. Thus, early detection on the other hand greatly improves the chances of survival rates in humans. At that place, Transfer Learning (TL) techniques have made significant improvements these days.

Material and Methods: We herein implemented the exploratory data analysis (EDA) technique to analyze 29 types of cancer deaths worldwide since 1990th century. Between them, we have emphasized lung cancer (LC) and colon cancers (CC) for our study and taken 25,000 histopathology image data from the publicly available Kaggle repository. Further, we proposed a novel methodology using the EfficientNetB7 model defining each step to classify five types of lung and colon tissues (two benign and three malignant) from the histopathological images. Although, an algorithm has been designed that clearly describes the workflow of our proposed method. This experiment has been done through input_shape=(X, Y, 3) on the 'ImageNet' dataset, Adam optimizer, and accuracy metrics using Python 3.8.8 software on Jupyter 6.4.3 environment.

Results: We evaluated the model progress using 50 epochs during the training phase, which resulted in more than 98% accuracy and less than 2% loss in both the training/ validation phases. Besides that, we designed a classification report that describes the performance of our model, where we achieved more than 98.07% accuracy score, 98% precision score, 98% of recall score, and 98% of f1-score. These results signify that implementing an optimization technique on the EfficientNetB7 model improves the overall performance as compared to 93.19% for LC 1 and 93.91% for CC 2 for the RestNet50 model.

Conclusion: A novelty of this research specifies the methodology to predict LC and CC by applying the EfficientNetB7 model to the cancer dataset which might be beneficial for both doctors as well as healthcare firms.

Keywords- World's Cancer death rate; Lung cancer; Colon cancer; Artificial intelligence; Transfer learning; EfficientNetB7; Adam optimizer

I. INTRODUCTION

In the last twenty years, the pathophysiologic mechanics of a variety of diseases were discovered, and new diagnostic procedures were devised in healthcare firms. A report by WHO states that in 2020, around 10 million deaths, or approximately one in six deaths, will be caused by cancer, making it the largest cause of death globally [3]. However, abnormal growth in any part of the human body can spread to the connecting organs beyond the boundaries. Early detection of cancer increases the chances

of successful treatment. The lower and upper estimates for 2017 range from 9.4 to 9.7 million according to the most recent Institute for Health Metrics and Evaluation (IHME) estimates, which places relatively narrow error margins around this global figure [4]. Thus, there is a need for a clear analysis of all cancers in the world to take necessary action against them. In this study, at first, we applied the EDA technique to visualize the number of people who died due to cancer diseases and also analyze the death percentage in each continent. A complete overview of the

data sources and procedures used to determine the global incidence and mortality estimates of cancer deaths from 1990 to 2019 is given in Figure 1, also following the cancer statistics update 5. This caused a rise from 1.1% - 1.15% each year.

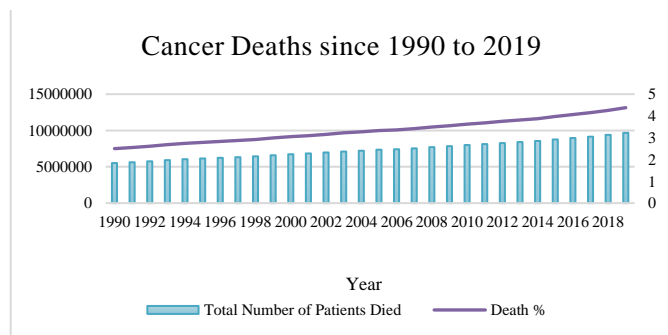


Figure 1. World's cancer death rate from 1990 to 2019

A statistical graph using the EDA technique has been designed that contains the total number of cancer deaths and their percentage as shown in Figure 2. It is visible that LC was leading as the topmost with 44801914 (i.e. 20.3%) and CC as 3rd most with 22857330 (i.e. 10.4%) cancer deaths followed by stomach cancer.

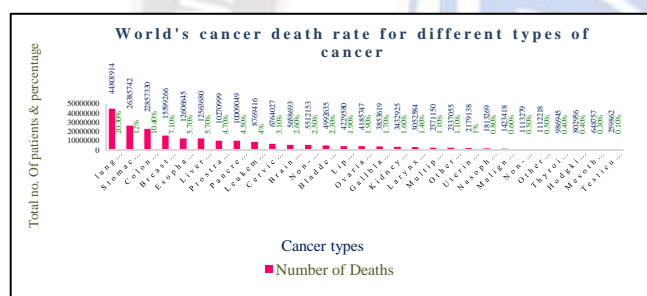


Figure 2. Fig. 2. Description of all 29 cancer deaths people and their percentages worldwide since the 1990 century

II. LITERATURE SURVEY

Among all those cancers, we herein emphasized on two most common cancers LC and CC, representing how these were mostly affected, causing a huge number of deaths globally since the 1990s century. Rather, some early malignancies may have detectable signs and symptoms, however, this is not always the case with LC and CC. In both men and women, LC is the second most frequent malignancy. It is the most common cancer that leads to death globally 6. As per the CDC, LC accounts for 80-90% of deaths related to cigarette smoking 7, but the most common type of LC is detected in people who don't smoke 8, 9. According to 2022 statistics CC is the 3rd most prevalent cancer in humans, which starts in the large intestine (colon) 10, 11. It usually begins as minor, non-malignant lumps of cells called polyps underneath the colon in older people, creating cancer over time. Major indications of this malignancy include rectal bleeding in the stool, gas or pain, weakness, and unexplained weight loss. Figure 3, shows the images of the lung & colon in the human body where cancer happens.

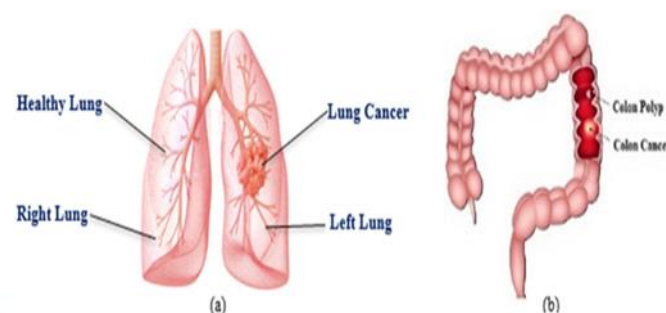


Figure 3. Fig. 3. Representing (a) Lung, and (b) Colon Cancer images of a human

Meanwhile, we also have designed a graph as shown in Figure 4, to represent the total number of people who died due to LC and CC in all continents from the year 1990 to 2019. In this study we found, Asia leads with the highest number of deaths in both LC and CC globally as compared to other continents.

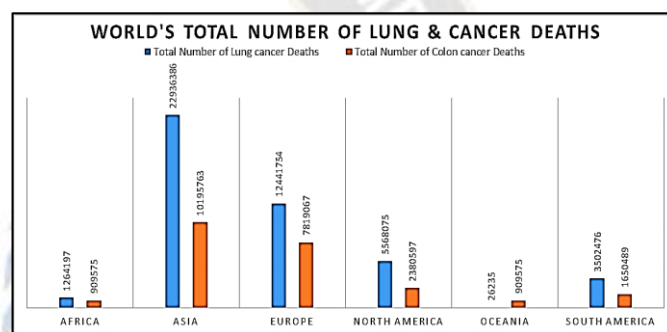


Figure 4. Fig. 4. World's cancer death rate due to LC and CC deaths from 1990 to 2019

However, in the last decades, Deep Learning (DL) has achieved greater success in the healthcare industries, helping people at an increased risk of cancer globally 12. DL in LC diagnosis supports a clinical decision-support system, which is the most common application for LC treatment these days 13-18. There is no denying that DL, particularly convolutional neural networks (CNN), excelled in classifying and recognizing patterns. It is difficult to create CNN from scratch. Building a successful layer selection and improving the result of CNN hyper-parameters takes a lot of time and effort. Additionally, we require a large volume of data (perhaps a few thousand) and strong computing (at least a high-performance GPU). Regardless, transfer learning (TL) another advancement in the medical field, only needs to retrain the fully linked layers depending on the problem. This appears to be a better option, especially in the absence of data and a graphical user unit (GPU). Thus, in this research work, we have gone with the TL model, namely EfficientNetB7 that creates a remedy for driver LC and CC on histopathological images. Besides that, we proposed a novel methodology that significantly describes each process to classify images into five different classes in our further section. This can effectively predict the disease at best accuracy even if there is less amount of data 19-22 and can aid in the detection of aberrant tissues in the lungs as well as in the colon 23, 24.

The main contributions of this study are:

- First, we analyze all 29 types of cancer death patients worldwide since 1990 century.
- Secondly, focused on lung and colon cancer deaths in all continents.
- Third, we implemented an image augmentation technique at the preprocessing stage to maximize the training data for our model.
- Proposed a novel method to predict five types of lung and colon cancers significantly.
- Build the EfficientNetB7 model after splitting data into train_set, test_set, and validation_set.
- Add 'Adam' as an optimizer, categorical_crossentropy as a loss function, and accuracy as a metric for our model compilation.
- Furthermore, implemented the EarlyStopping () method to remove overfitting issues.
- We trained the model with 50 epochs and found 98.47 % as training accuracy and 98.04% as validation accuracy.
- Finally, we plot training/validation loss/accuracy using a line graph and classification report using a confusion matrix for all five types of cancers.

The rest of the paper is as follows: Section 2, shows the material and methods for our study; Section 3, gives the experimental result; Section 4, describes the findings throughout our study; and the end Section 5, concludes with a conclusion.

III. MATERIAL AND METHODS

The accuracy of prediction is critical in medical image analysis. The quantity and quality of medical imagery datasets are vital to using Machine Learning (ML) and Deep Learning (DL) to ensure the accuracy of future predictions. LC screening using Low Dose CT provides clinical developments for a large volume of people around the world [25, 26, 27]. DL's transfer learning principle allows the models to be adapted to specific application requirements. Because these models have already been trained on ImageNet, to boost overall performance and reduce computing complexity [20, 28]. TL eliminates the need for a big dataset to a greater extent, as well as the training cost and computation costs. AlexNet, LeNet, MobileNet, GoogleNet, and more pre-trained models are available. Thus, in this article, a novel methodology has been proposed for predicting both LC and CC, as shown in Figure 5. Although, it includes an introduction to DL, as well as a TL-based model named, EfficientNetB7 architecture for detecting the most common five types of LC and CC from image datasets.

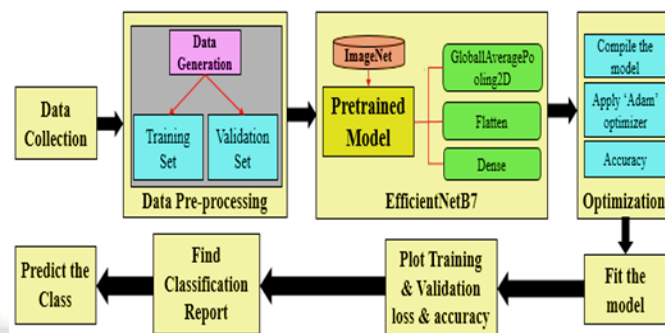


Figure 5. Proposed Methodology Design to Classify LC & CC

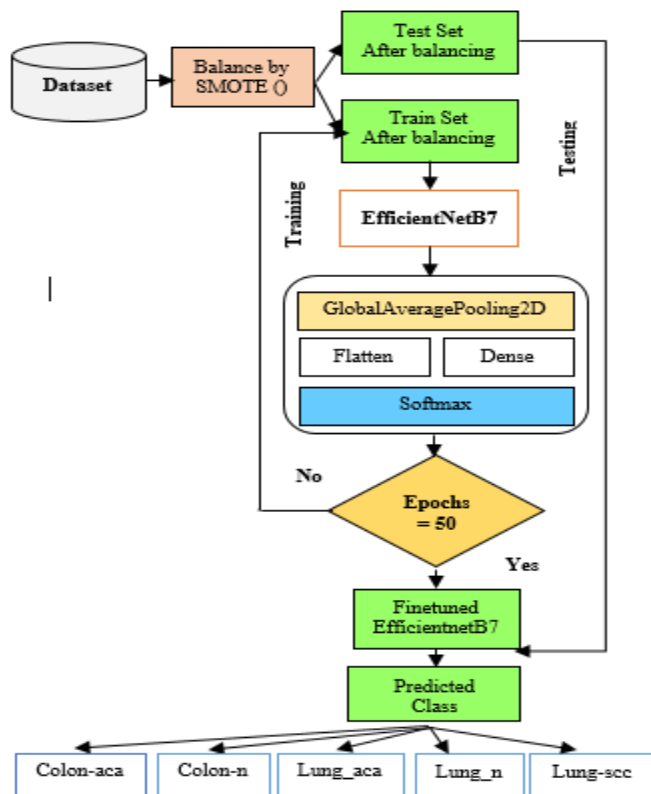
Algorithm

Input: Histopathology images

1. Collect the image dataset.
2. Preprocess all images and convert them into 224*224*3 format.
3. Generating dataset as 80% for training and 20% for validation using ImageDataGenerator and set batch_size = 128.
4. Fed these preprocessed images into a model
5. Collect weights with input_shapes = (X, Y, 3) from the ImageNet.
6. Apply the compound scaling method on images to uniformly scale the dimension of the network.
7. Apply the grid search method to the above result to get the relationship between them.
8. Find suitable scaling coefficients for every dimension.
9. Select the baseline network to design neural networks
10. Compile the model and set optimizer = Adam.
11. Fit the model and set callbacks = [early_stopping].
12. Train & validate the model with a set of epochs.
13. Plot training & validation accuracy/loss for the model.
14. Predict the model on a validation set of data.
15. Find the classification_report using sklearn.metrics.
16. Plot confusion_matrix, containing the true & predicted values.

Result: accuracy result

Flowchart: Process workflow of the proposed algorithm using the EfficientNetB7 TL model



A. Material

Collecting data allows us to maintain previous events and utilize data analysis to uncover repeating trends. Moreover, creating predictive models by utilizing DL algorithms based on those patterns, may benefit doctors and predict future changes. As a result, gathering data to train our model is the first stage in the DL process. Any DL model's predictions are only as good as the data it was trained on. Although, for constructing high-performing models, good data collection (i.e., error-free and including important information) procedures are critical. This LC and CC dataset includes 25,000 histopathology images divided into five classes. Images are arranged with 768 by 768 pixels for further pre-processing and to validate the sources 29. There are 500 total images of colon tissue (250 benign and 250 adenocarcinomas) and 750 complete images of lung tissue (250 benign, 250 adenocarcinomas, and 250 squamous cell carcinomas) that have been augmented to 25,000.

B. Method

1) Data Pre-processing

Data Pre-processing is the crucial step after collecting data in an ML algorithm. It includes data cleaning, transforming categorical values into numerical values, and identifying missing/null values before going into the model. Thus it follows some basic steps as follows:

- Handling missing values and categorical values.
- Convert these values into numerical types.
- Implement the EDA statistical approach by designing summarized graphs to analyze the data and to find the patterns between the variables.
- Split the training data into two or more sets to train and evaluate the model with a single source of data.

- Train and validation folders in an 80:20 ratio.
- Apply feature scaling

In this LC and CC dataset, each folder includes five subfolders, one for each of the classes. To load the images, we have used the ImageDataGenerator class, using the flow from the directory function to generate batches of images and labels. The training set has 20,000 images from five classes, whereas the validation set contains 5,000 images from five classes. However, the EfficientNet models are typically either excessively deep or extremely reasonably high. Meanwhile, the compound scaling (CS) method has been used to balance the dimensions of width (w), depth (d), and resolution (r) by scaling them with a constant ratio. It is mathematically defined by the three most common constraints alpha, beta, and gamma, which are exponentiated by 'φ', representing the rise in the processing ability of the network.

$$\begin{aligned} d &= \alpha^\phi \\ w &= \beta^\phi \\ r &= \gamma^\phi \end{aligned} \quad (1)$$

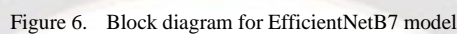
$$\begin{aligned} \text{s.t. } &\alpha \cdot \beta^2 \cdot \gamma^2 \approx 2 \\ &\alpha, \beta, \text{ and } \gamma \geq 1 \end{aligned}$$

Here, α, β, and γ are the constant coefficients. The biggest advancement of CS is to improve the accuracy by 2.5% as compared to 1-dimension scaling methods. Thus, in this paper, we have taken an EfficientNetB7 model that works on the CS method to provide greater accuracy while predicting LC and CC.

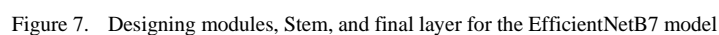
2) Model Design

As part of lung and colon cancer statistics till 2019, there is a requirement for successful evaluation of this cancer at the initial stage. Thus, the application of a good model can fulfill the needs of the physicians and can take necessary action against them. A TL model with a smaller number of parameters has been designed over here that has already been pre-trained with millions of images containing weights from the ImageNet dataset. As the name suggests, EfficientNetB7 contains 7 blocks and 813 layers to extract the features from the images. In each block, modules are added to move forward to the next block, as shown in Figure 6. This process includes some basic steps as follows:

- At each module, layers are activated to filter the images that are fed into the next layer.
- At the input end, the GlobalAveragePooling2D layer applies average pooling on spatial data until each spatial dimension becomes 1.
- In the middle, a flattened layer is used that converts the image into a 1-dimensional array to feed into the next layer.
- At the output end, two dense layers are imported with the Rectified Linear unit (ReLU) activation function that collects neurons from previous layers and ReLU implies not stopping forward negative values in the network.
- This model uses three modules, one stem, and one final layer to complete its whole process, as described in Figure 7.



Module 2 — contains the beginning of all seven blocks despite the first block.



An optimizer is a tool or method that optimizes neural network (NN) properties like weights and learning rates. As a result, it aids in decreasing total loss and raising accuracy. To

unique learning rates for each parameter. It scales the learning rate using squared gradients and benefits from momentum by using the gradient's time series despite the gradient itself.

$$me_n = P[I^n] \quad (2)$$

Where, me = moment estimation

n = number of me for independent variables (I)

P = Predicted value

However, a better understanding of the model is to predict the moments. The reason for that is that 'adam' uses moving averages (i.e. d and a), hyper-parameters as 'h', and gradients as 'g' on a group of variables. These have default values of 0.9 and 0.99. This can be represented as:

$$d_t = h_1 d_{t-1} + 1 - h_1 \quad (3)$$

$$a_t = h_2 d_{t-1} + 1 - h_2 g_t^2 \quad (4)$$

Moreover, the predicted value for moving variables always has to be equal to the parameters, defined as unbiased. It follows the calculation as:

$$P[d_t] = P[g_t] \quad (5)$$

$$P[a_t] = P[g_t^2] \quad (6)$$

But, this will not happen as true, if we assign the value as '0' to the moving variables i.e. d_t = a_t = 0, as defined in eq. (7). The predicted value for the moment variable as 'd' has newly formed and displayed in eq. (8) as:

$$d_t = (1 - h_1) \sum_{x=0}^t h_1^{t-x} g_x \quad (7)$$

$$P[d_t] = P[g_x](1 - h_1^t) + \vartheta \quad (8)$$

In this eq. (8), the predicted value approximates the value of g[x] with g[t] and also calculates the sum as it has not further depended on 'x'. As we discussed, the approximation has been made, so an error 'ϑ' has been initiated in this formula. As the value for 'ht' is moving forward to '0', there is the need to find a good estimator that will predict the value to '1', according to our requirement. So, the new formula for the predictor after modifying the bias is:

$$Exp(d) = \frac{d_t}{1 - h_1^t} \quad (9)$$

$$Exp(a) = \frac{a_t}{1 - h_2^t} \quad (10)$$

Where,

Exp(d) and Exp(a) = Estimated moment variables

Now, it is time to modify the attributes of our models like weight (w) and learning rate (lr) to minimize the loss and increase the accuracy. So the updated formula for 'w' is as follows:

$$w_t = w_{t-1} - \rho \frac{Exp(d)_t}{\sqrt{Exp(a)_t + \varepsilon}} \quad (11)$$

Where,

ρ = number of iterations

$$\varepsilon = \text{loss}$$

The primary need of an ML algorithm is to fit the best weights and biases to minimize the loss over the prediction range. It is the process of feeding training data to an ML algorithm so that it can learn. The model's effectiveness during training will ultimately decide how well it will perform when it is implemented into a user-friendly application. The model.fit () evaluates the capacity to adapt data equivalent to that with which it was trained. Here, we add ReLU activation layers at the end to minimize the output parameters and softmax layer to classify the cancers. The Dense has 128 nodes in the second layer and 64 nodes in the third layer. However, we define Adam optimizer and categorical cross entropy as loss functions in this work. The model has been trained with 50 epochs. A good model tends to provide accuracy on unrevealed inputs that imitate the output so closely. Moreover, early_stopping () has been taken to avoid overfitting issues during the training phase 31.

IV. RESULTS ANALYSIS

We herein implemented the model.accuracy () function to design training/validation accuracy/loss plots for the EfficientNetB7 model. This resulted in above 98.07% of accuracy and below 2% of loss, as given in Figure 8. In most cases, it's given as a percentage. It provides all the respective true predictions resulting in true or false. Loss is more difficult to interpret than accuracy. A loss function determines the possibility of uncertainty in the prediction that describes the difference from the true value. The purpose of the training procedure is to reduce the loss value. The two most common loss functions named Logloss () and cross_entropy_loss () have been implemented here, representing the error rates between '0' and '1' 32. The training & validation accuracy and loss of our model have been designed as follows in this section. All these experiments have been done using Python 3.8.8 software on Jupyter Notebook 6.4.3 platform.

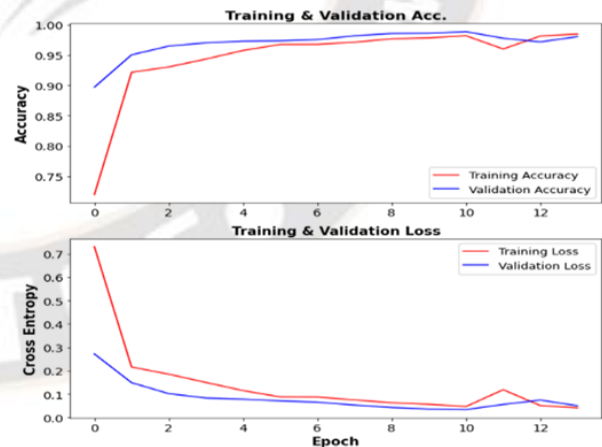


Figure 8. Training & Validation Accuracy/Loss for EfficientNetB7 model

However, designing a confusion matrix (cm) shows how well our model performs on a set of test data while predicting LC and CC 33. Thus, in this study, we analyze our model performances using some common metrics such as recall (R), specificity (S), accuracy (A), and precision (P). These are calculated from True Positives (TP), False Positives (FP), True Negatives (TN), and False Negatives (FN), as resulted in the

confusion matrix in Table 1. Besides that, we have designed a comparison table to differentiate the performance of our proposed method from previously found existing methods in both lung and colon cancer areas, as shown in below Table 2.

- TP defines the total number of actual predictions in classifying the disease.
- TN defines the total number of negative predicted values corresponding to an actual class.
- FP defines the total number of true predicted values in correspond to the negative class, sometimes called a Type-1 error.
- FN defines the false predicted values on the actual class, also called a Type-2 error.

However, to find the performance of our model, we perform two strategies: classification accuracy, and classification report.

- Classification Accuracy: a common and widely accepted metric for 2-class problems. It is obtained by dividing the total number of classified correctly outcomes by all the occurrences. It is classified as:

$$A = \frac{TP+TN}{TP+FP+FN+TN} \quad (12)$$

- Classification Report: It measures the reliability of our model, by calculating these P, R, F1Score, and support.

- P is calculated by dividing TP by the total of TP and FP which gives the number of correct predictions found to be positive.

$$P = \frac{TP}{TP+FP} \quad (13)$$

- R is calculated by dividing TP by the total of TP and FN that are correctly predicted.

$$R = \frac{TP}{TP+FN} \quad (14)$$

- F1Score is calculated by dividing the precision by recall.

$$F1 - score = \frac{2*(P*R)}{P+R} \quad (15)$$

- Support gives the correct results that come into a class either '0' or '1'.

Furthermore, Table 1 represents the performance metric for all five types of lung and colon tissues. Additionally, Figure 9 shows the result of normalized cm after evaluating our model successfully.

TABLE I. PERFORMANCE METRIC FOR ALL FIVE TYPES OF LUNG AND COLON TISSUES

	Precision	Recall	F1-score	Support
0	1.00	0.96	0.98	1000
1	0.98	1.00	0.99	1000
2	0.94	0.98	0.96	1000
3	1.00	1.00	1.00	1000
4	0.98	0.96	0.97	1000
accuracy			0.98	5000
macro avg	0.98	0.98	0.98	5000
weighted avg	0.98	0.98	0.98	5000

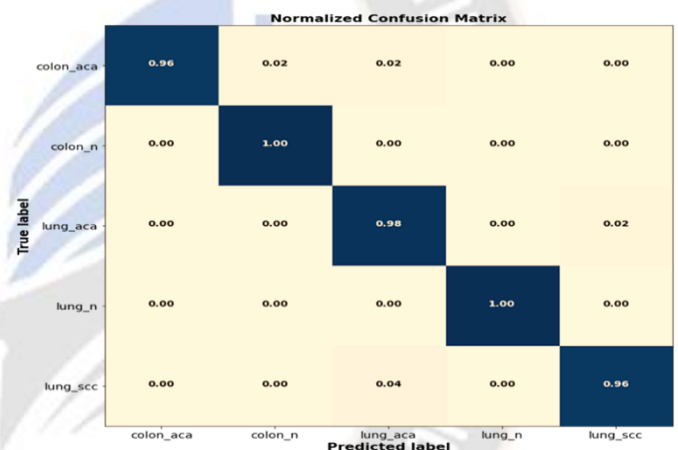


Figure 9. Normalized Confusion_matrix for all five lung & colon tissues

TABLE 2. DESCRIPTION OF THE DATASET, CANCER TYPE, MODELS IMPLEMENTED, AND PERFORMANCE METRICS FOR THE PROPOSED MODEL WITH PREVIOUSLY PUBLISHED RESEARCH IN LUNG AND COLON CANCER DIAGNOSIS

Author	Cancer Type	Dataset	Image Collected	Techniques Used	Accuracy (%)	Precision	Recall	Sensitivity	Specificity	F1-Score
Nobrega et al. ¹	Lung	CT Images	CT Scans	ResNet50 SVM RBF	93.19	-	-	-	-	-
Bukhari et al. ²	Colon	Histopathology images	Colonoscopy	ResNet50	93.91	-	-	-	-	-
Suresh et al. ³⁴	Lung	Consortium public repository	CT Scan	CNN	93.90	-	-	93.40	93.00	-
Shakeel et al. ³⁵	Lung	ELVIRA Biomedical Data Set	CT Scan	GACNN	94.17	95.67	95.82	95.82	-	95.74
Yuan et al. ³⁶	Colon	Real-time colonoscopy video database	Colonoscopy	AlexNet	91.47	-	-	-	-	-
Babu et al. ³⁷	Colon	Real-time images from Aster Medcity, Kochi, India	Biopsy	RF	85.30	-	-	-	-	85.20

Akbari <i>et al.</i> ³⁸	Colon	Asu Mayo Test Clinic database	Colonoscopy	CNN	90.28	74.34	68.32	-	94.97	-
Masood <i>et al.</i> ³⁹	Lung	LIDC-IDRI database, LUNA 2016 Dataset	CT Scan	DFCNet	96.33	-	-	83.67	96.17	-
Shen <i>et al.</i> ⁴⁰	Lung	LC25000	CT Scan	ML-CNN	87.14	-	-	77.00	93.00	-
Fillo <i>et al.</i> ⁴³	Lung	LC25000	CT Scans	CNN	92.63	-	-	-	-	-
Hatuwal <i>et al.</i> ⁴⁴	Lung & Colon	LC25000	Histopathological	CNN	96.33	96.39	96.37	-	-	96.38
Proposed Method	Lung & Colon	LC25000	Histopathological	EfficientNetB7	98.07	98.00	98.00	96.00	98.57	98

V. DISCUSSION

As discussed previously in Figure 1, the total number of deaths due to cancers has become a global concern since the 1990 century. In addition, Figure 2 comprises the total number of people who died from 29 cancers, where we found LC leads with 1st and CC as 3rd most cancer deaths. The most fatal cancer in the world is LC [4]. Due to the late stage of diagnosis, where treatments are less successful than at earlier stages, and the ongoing rise in LC incidence, the 5-year survival rate is only 20% (De Angelis et al. 2014). Also, clinically it was found that CC had made a great impact with 10.4 % of deaths globally.

Additionally, we have designed a graph that replicates the total number of deaths due to LC and CC in each continent, as shown in Figure 4. This graph displays LC in blue color and CC in orange color. Furthermore, we have applied the optimization technique on a TL method to determine the risk of death and to predict these cancers from histopathological images in our next Figure 5.

In contrast to all developments in the healthcare field, DL has been highly considered in the field of AI, it requires a lot of data and effort. A deep learning-based framework to classify the five types of LC and CC gives an accuracy of 96.33% [45] and 94.6% [46]. Thus, we tried an EfficientNetB7 model for our proposed method as this model works well on lung and colon images to identify the disease more efficiently [47]. Each block comprises three modules that we have discussed in Figures 6 and 7.

For this experiment, we have designed a flowchart, where each step describes the process of classifying five types of lung and colon cancers. The training/validation loss/accuracy performance result has been displayed in Figure 8 and also we designed a normalization confusion matrix for our model. After successful evaluation, our proposed model gives an accuracy of 98.07% that aims to overcome the shortcomings of DL. However, an ensemble TL model for predicting LC gives an accuracy of 91% which is less than our proposed model [48]. Besides that, we finally compare our model performance result with previous research findings, where we found better than others.

VI. CONCLUSION

In the past few years, deep learning has made huge advancements in the healthcare field. Thus, in this article, we have taken a DL-based model, called EfficientNetB7 which effectively work on lung & cancer dataset. This model improves accuracy and efficiency by eliminating the parameter size over the DL models. This model works well on a small dataset like over here (i.e. consisting of 25,000 images), to predict the

disease effectively. Although, a methodology has been proposed that takes some basic steps for implementing this model over here. Two measure parameters i.e. accuracy and loss function are used for evaluating this model's performance. And finally, a table has been designed that represents the key features to measure the performance by using confusion_matrix. At last, it was found that our proposed model finds a good accuracy result of 98% when predicting LC and CC in humans. The important contribution of our study was described as follows:

- First, apply the EDA technique to visualize the cancer death people
- EfficientNetB7 works well on ImageNet, where they are most applicable, and also apply to other datasets.
- Reduces parameter size and FLOPS by a significant amount while offering larger accuracy and better efficiency than recent CNNs.
- This proposed model in particular outperforms even the predefined CNN and VGG models, achieving new state-of-the-art 98% accuracy.
- We anticipate that EfficientNetB7 could potentially serve as a new basis for upcoming computer vision activities in healthcare organizations by offering substantial increases to model effectiveness.

However, this research found some limitations like as an increased amount of data flow and considerably less processing than other networks for this method. Thus, this model suffers from low hardware accelerators such as GPU. Other challenges are fewer parameters require increased numbers of channels to improve the model accuracy. In contrast to all those issues, this model might help the doctors as well as the patient to identify the cancers in the beginning stages, so that they will be aware and take necessary actions to avoid unnecessary deaths in the future days. Although, we have planned to add new features to our model to predict the diseases significantly. Furthermore, shortly, we will go with real-time medical data and implement our model with them.

DECLARATION

A. Funding

The authors received no financial support for the research, authorship, and/or publication of this article.

B. Conflict of interest

On behalf of all authors, the corresponding author states that there is no conflict of interest.

C. Availability of data and materials

This Lung and Colon cancer dataset has been collected from a freely available Kaggle repository. Source Link as:

<https://www.kaggle.com/datasets/andrewmvd/lung-and-colon-cancer-histopathological-images>

REFERENCES

- [1] da Nóbrega, RVM, Rebouças Filho, PP, Rodrigues, MB, et al. Lung nodule malignancy classification in chest computed tomography images using transfer learning and convolutional neural networks. *Neural Comput. Appl.* 2020, 32, 11065–11082. <https://doi.org/10.1016/j.patcog.2016.05.029>.
- [2] Bukhari, SUK, Asmara, S, Bokhari, SKA, et al. The Histological Diagnosis of Colonic Adenocarcinoma by Applying Partial Self Supervised Learning. *medRxiv* 2020. doi: <https://doi.org/10.1101/2020.08.15.20175760>
- [3] <https://www.who.int/news-room/fact-sheets/detail/cancer>.
- [4] Ferlay, J, Colombet, M, Soerjomataram, I, et al. Estimating the global cancer incidence and mortality in 2018: GLOBOCAN sources and methods. *International journal of cancer*, 144(8), 1941–1953. <https://doi.org/10.1002/ijc.31937>
- [5] <https://www.kaggle.com/code/sandraasagade/cancer-death-rates-eda-1990-2019/data?select=total-cancer-deaths-by-type.csv>.
- [6] Thandra KC, Barsouk A, Saginala K, et al. Epidemiology of lung cancer. *Contemporary Oncology*, 2021, 25(1), 45. <https://doi.org/10.5114/wo.2021.103829>.
- [7] https://www.cdc.gov/cancer/lung/basic_info/risk_factors.htm
- [8] Wu F, Fan J, He Y, et al. Single-cell profiling of tumour heterogeneity and the microenvironment in advanced non-small cell lung cancer. *Nature Communications*, 2021, 12(1), 1–11. <https://doi.org/10.1038/s41467-021-22801-0>.
- [9] Mathios D, Johansen, JS, Cristiano S, et al. Detection and characterization of lung cancer using cell-free DNA fragmentomes. *Nature Communications*, 2021, 12(1), 1–14. <https://doi.org/10.1038/s41467-021-24994-w>.
- [10] Prusty, S et al. Prediction of Breast Cancer Using Integrated Machine Learning-fuzzy and Dimension Reduction Techniques. vol. 45, no. 1, pp. 1633–1652, 2023.
- [11] Irrazabal T, Thakur BK, Croitoru K, et al. Preventing colitis-associated colon cancer with antioxidants: A systematic review. *Cellular and Molecular Gastroenterology and Hepatology*, 2021, 11(4), 1177–1197. <https://doi.org/10.1016/j.jcmgh.2020.12.013>.
- [12] Togacar M, Disease type detection in lung and colon cancer images using the complement approach of inefficient sets. *Computers in Biology and Medicine*, 2021, 137, 104827. <https://doi.org/10.1016/j.combiomed.2021.104827>.
- [13] Zhang K, Chen K, Artificial intelligence: opportunities in lung cancer. *Current Opinion in Oncology*, 2022, 34(1), 44–53. DOI: <https://doi.org/10.1097/CCO.0000000000000796>.
- [14] Christie JR, Lang P, Zelko LM, et al. Artificial intelligence in lung cancer: bridging the gap between computational power and clinical decision-making. *Canadian Association of Radiologists Journal*, 202172(1), 86–97. <https://doi.org/10.1177/0846537120941434>.
- [15] Yang H, Chen, L., Cheng, Z., et al. Deep learning-based six-type classifier for lung cancer and mimics from histopathological whole slide images: a retrospective study. *BMC Medicine*, 2021, 19(1), 1–14. <https://doi.org/10.1186/s12916-021-01953-2>.
- [16] Tunali I, Gillies RJ, Schabath MB, Application of radiomics and artificial intelligence for lung cancer precision medicine. *Cold Spring Harbor perspectives in medicine*, 2021, 11(8), a039537. doi: 10.1101/cshperspect.a039537.
- [17] Prusty, S, Dash, SK, Patnaik S, Prusty, SG.P, Tripathy, N, EPD: an integrated modeling technique to classify BC. In 2023 International Conference in Advances in Power, Signal, and Information Technology (APSIT) (pp. 651–655). IEEE.
- [18] Baranwal N, Doravari P, Kachhoria R, Classification of Histopathology Images of Lung Cancer Using Convolutional Neural Network (CNN), arXiv preprint arXiv: 2112.13553, 2021. <https://doi.org/10.48550/arXiv.2112.13553>.
- [19] Prusty S, Patnaik S, Dash SK, SKCV: Stratified K-fold cross-validation on ML classifiers for predicting cervical cancer. *Frontiers in Nanotechnology*, 2022, 4, 972421.
- [20] Shinde S, Kulkarni U, Mane D, et al. Deep learning-based medical image analysis using transfer learning. In *Health Informatics: A Computational Perspective in Healthcare*, 2021, (pp. 19–42). Springer, Singapore. https://doi.org/10.1007/978-981-15-9735-0_2.
- [21] Gao J, Jiang Q, Zhou B, et al. Lung Nodule Detection using Convolutional Neural Networks with Transfer Learning on CT Images. *Combinatorial Chemistry & High Throughput Screening*, 2021, 24(6), 814–824. DOI: <https://doi.org/10.2174/1386207323666200714002459>.
- [22] Prusty S, Dash SK, Patnaik S, A Novel Transfer Learning Technique for Detecting Breast Cancer Mammograms Using VGG16 Bottleneck Feature. *ECS Transactions*, 2022, 107(1), 733. <https://doi.org/10.1149/10701.0733ecst>.
- [23] Lee ALS, To CCK, Lee ALH, et al. Model architecture and tile size selection for convolutional neural network training for non-small cell lung cancer detection on whole slide images. *Informatics in Medicine Unlocked*, 2022, 100850. <https://doi.org/10.1016/j.imu.2022.100850>.
- [24] Silva F, Pereira T, Morgado J, et al. EGFR assessment in lung cancer CT images: Analysis of local and holistic regions of interest using deep unsupervised transfer learning. *IEEE Access*, 2021, 9, 58667–58676. doi: 10.1109/ACCESS.2021.3070701.
- [25] Oudkerk M, Liu S, Heuvelmans MA, et al. Lung cancer LDCT screening and mortality reduction—evidence, pitfalls and future perspectives. *Nature Reviews Clinical Oncology*, 2021, 18(3), 135–151. <https://doi.org/10.1038/s41571-020-00432-6>.
- [26] Hu L, Lin JY, Sigel K, et al. Estimating heterogeneous survival treatment effects of lung cancer screening approaches: A causal machine learning analysis. *Annals of Epidemiology*, 2021, 62, 36–42. <https://doi.org/10.1016/j.annepidem.2021.06.008>.
- [27] Han Y, Ma Y, Wu Z, et al. Histologic subtype classification of non-small cell lung cancer using PET/CT images. *European journal of nuclear medicine and molecular imaging*, 2021, 48(2), 350–360. <https://doi.org/10.1007/s00259-020-04771-5>.
- [28] Zhu W, Braun B, Chiang LH, et al. Investigation of transfer learning for image classification and impact on training sample size. *Chemometrics and Intelligent Laboratory Systems*, 2021, 211, 104269. <https://doi.org/10.1016/j.chemolab.2021.104269>.
- [29] Borkowski AA, Bui MM, Thomas LB, et al. Lung and Colon Cancer Histopathological Image Dataset (LC25000), 2019. <https://doi.org/10.48550/arXiv.1912.12142>
- [30] Li P, He X, Song D, et al. Improved Categorical Cross-Entropy Loss for Training Deep Neural Networks with Noisy Labels. In *Chinese Conference on Pattern Recognition and Computer Vision (PRCV)*, 2021, (pp. 78–89). Springer, Cham. https://doi.org/10.1007/978-3-030-88013-2_7
- [31] Bentoumi, M, Daoud, M, Benaouali, M, et al. Improvement of emotion recognition from facial images using deep learning and early stopping cross-validation. *Multimed Tools Appl.*, 2022, 81, 29887–29917. <https://doi.org/10.1007/s11042-022-12058-0>.
- [32] Gulum MA, Trombley CM, Kantardzic M, et al. A Review of Explainable Deep Learning Cancer Detection Models in Medical Imaging. *Applied Sciences*, 2021, 11(10), 4573. <https://doi.org/10.3390/app11104573>
- [33] Talukder, MA, Islam, MM, Uddin, MA, et al. Machine learning-based lung and colon cancer detection using deep feature extraction and ensemble learning. *Expert Systems with Applications*, 2022, 117695. <https://doi.org/10.1016/j.eswa.2022.117695>.
- [34] Suresh, S, Mohan, S, ROI-based feature learning for efficient true positive prediction using convolutional neural network for lung cancer diagnosis. *Neural Comput. Appl.* 2020. <https://doi.org/10.1007/s00521-020-04787-w>.
- [35] Shakeel, PM, Tolba, A, Al-Makhadmeh, Z et al. Automatic detection of lung cancer from biomedical data set using discrete AdaBoost optimized ensemble learning generalized neural networks. *Neural Comput & Applic* 32, 2020, 777–790. <https://doi.org/10.1007/s00521-018-03972-2>.
- [36] Yuan, Z, Izadyazdanabadi, M, Mokkapat, D, et al. Automatic polyp detection in colonoscopy videos. *Med. Imaging 2017 Image Process.* 2017, 10133, 101332K. <https://doi.org/10.1117/12.2254671>.
- [37] Babu, T, Gupta, D, Singh, T, et al. Colon Cancer Prediction on Different Magnified Colon Biopsy Images. In *Proceedings of the 10th International Conference on Advanced Computing (ICoAC)*,

- Chennai, India, 13–15 December 2018, pp. 277–280. DOI: 10.1109/ICoAC44903.2018.8939067.
- [38] Akbari, M, Mohrekesh, M, Rafiei, S, et al. Classification of Informative Frames in Colonoscopy Videos Using Convolutional Neural Networks with Binarized Weights. In Proceedings of the Annual International Conference IEEE Engineering in Medicine and Biology Society (EMBS), Honolulu, Hawaii, 17–22 July 2018; pp. 65–68. DOI 10.1109/EMBC.2018.8512226.
- [39] Masood, A, Sheng, B, Li, P, et al. Computer-Assisted Decision Support System in Pulmonary Cancer Detection and stage classification on CT Images. *J. Biomed. Inform.* 2018, 79, 117–128. <https://doi.org/10.1016/j.jbi.2018.01.005>.
- [40] Shen, W, Zhou, M, Yang, F, et al. Multi-crop convolutional neural networks for lung nodule malignancy suspiciousness classification, *Pattern Recognit.*, vol. 61, pp. 663–673, Jan. 2017.
- [41] De Carvalho Filho, AO, Silva, AC, de Paiva, ACR, et al. Classification of patterns of benignity and malignancy based on CT using topology-based phylogenetic diversity index and convolutional neural network, *Pattern Recognit.*, vol. 81, pp. 200–212, Sep. 2018.
- [42] Hatuwal, BK, Thapa, HC, Lung cancer detection using convolutional neural network on histopathological images. *Int. J. Comput. Trends Technol.*, 2020, 68(10), 21–24. 10.14445/22312803/IJCTT-V68I10P104.
- [43] Tan M, Le Q. EfficientNet: Rethinking model scaling for convolutional neural networks. In International conference on machine learning, 2019, (pp. 6105–6114). PMLR. <http://proceedings.mlr.press/v97/tan19a/tan19a.pdf>.
- [44] Masud M, Sikder N, Nahid AA, A machine learning approach to diagnosing lung and colon cancer using a deep learning-based classification framework, *Sensors*, 2021, 21(3):748. <https://doi.org/10.3390/s21030748>.
- [45] Hlavcheva D, Yaloveha V, Podorozhniak A, Comparison of CNNs for Lung Biopsy Images Classification. In 2021 IEEE 3rd Ukraine Conference on Electrical and Computer Engineering (UKRCON) 2021 Aug 26 (pp. 1–5). IEEE. doi: 10.1109/UKRCON53503.2021.9575305
- [46] Phankokkruad M, Ensemble transfer learning for lung cancer detection. In 2021 4th International Conference on Data Science and Information Technology 2021 Jul 23 (pp. 438–442). <https://doi.org/10.1145/3478905.3478995>.